

**Ground-state phases of the frustrated spin- $\frac{1}{2}$ J_1 - J_2 - J_3 Heisenberg
ferromagnet ($J_1 < 0$) on the honeycomb lattice with $J_3 = J_2 > 0$**

P. H. Y. Li and R. F. Bishop

*School of Physics and Astronomy, Schuster Building,
The University of Manchester, Manchester, M13 9PL, UK*

D. J. J. Farnell

*Division of Mathematics, Faculty of Advanced Technology,
University of Glamorgan, Pontypridd CF37 1DL, Wales, UK*

J. Richter

*Institut für Theoretische Physik, Otto-von-Guericke Universität Magdeburg,
P.O.B. 4120, 39016 Magdeburg, Germany*

C. E. Campbell

*School of Physics and Astronomy, University of Minnesota,
116 Church Street SE, Minneapolis, Minnesota 55455, USA*

Abstract

We study the ground-state (gs) properties of the frustrated spin- $\frac{1}{2}$ J_1 - J_2 - J_3 Heisenberg model on the two-dimensional honeycomb lattice with ferromagnetic nearest-neighbor ($J_1 = -1$) exchange and frustrating antiferromagnetic next-nearest-neighbor ($J_2 > 0$) and next-next-nearest-neighbor ($J_3 > 0$) exchanges, for the case $J_3 = J_2$. We use the coupled-cluster method implemented to high orders of approximation, complemented by the Lanczos exact diagonalization of a large finite lattice with 32 sites, in order to calculate the gs energy, magnetic order parameter, and spin-spin correlation functions. In one scenario we find a quantum phase transition point between regions characterized by ferromagnetic order and a form of antiferromagnetic (“striped”) collinear order at $J_2^c \approx 0.1095 \pm 0.0005$, which is below the corresponding hypothetical transition point at $J_2^{\text{cl}} = \frac{1}{7}$ (≈ 0.143) for the classical version of the model, in which we momentarily ignore the intervening noncollinear spiral phase in the region $\frac{1}{10} < J_2 < \frac{1}{5}$. Hence we see that quantum fluctuations appear to stabilize somewhat the collinear antiferromagnetic order in preference to the ferromagnetic order in this model. We compare results for the present ferromagnetic case (with $J_1 = -1$) to previous results for the corresponding antiferromagnetic case (with $J_1 = +1$). The magnetic order parameter is found to behave similarly for the ferromagnetic and the antiferromagnetic models for large values of the frustration parameter J_2 . However, there are considerable differences in the behavior of the order parameters for the two models for $J_2/|J_1| \lesssim 0.6$. For example, the quasiclassical collinear magnetic long-range order for the antiferromagnetic model (with $J_1 = +1$) breaks down at $J_2^{c2} \approx 0.60$, whereas the “equivalent” point for the ferromagnetic model (with $J_1 = -1$) occurs at $J_2^c \approx 0.11$. Unlike in the antiferromagnetic model (with $J_1 = +1$), where a plaquette valence-bond crystal phase intrudes between the two corresponding quasiclassical antiferromagnetic phases (with Néel and striped order) for $J_2^{c1} < J_2 < J_2^{c2}$, with $J_2^{c1} \approx 0.47$, we find no clear indications at all in the ferromagnetic model for an intermediate magnetically disordered phase between the corresponding phases exhibiting ferromagnetic and striped order. Instead the evidence for the ferromagnetic model (with $J_1 = -1$) points to one of two scenarios: either there is a direct first-order transition between the two magnetically ordered phases, as mentioned above; or there exists an intervening phase between them in the very narrow range $0.10 \lesssim J_2 \lesssim 0.12$, which is probably a remnant of the spiral phase that exists in the classical counterpart of the model over the larger range $\frac{1}{10} < J_2 < \frac{1}{5}$.

PACS numbers: 75.10.Jm, 75.30.Gw, 75.40.-s, 75.50.Ee

I. INTRODUCTION

In recent years frustrated quantum spin systems on regular two-dimensional (2D) lattices have aroused a great deal of research interest.^{1–3} In particular the interplay of magnetic frustration and quantum fluctuations has been seen to be a very effective route to destabilize or destroy magnetic order and thereby to create new quantum phases. Such 2D magnetic systems can thus in turn develop a diverse array of phases with widely different ordering properties, such as antiferromagnets with quasiclassical Néel ordering, quantum “spirals”, valence-bond crystals/solids, phases with nematic ordering, and spin liquids. Other factors that influence the ground-state (gs) phase structures are the nature of the underlying crystallographic lattice, the number and nature of the bonds on this lattice, and the spin quantum numbers of the atoms localized to the sites on the lattice. The theoretical investigation of these models has proceeded hand in hand with the discovery and experimental investigation of ever more quasi-2D magnetic materials with novel properties.

One of the most intensively studied of all of the frustrated 2D models is the spin- $\frac{1}{2}$ J_1 - J_2 Heisenberg antiferromagnet (HAF) on the square lattice with nearest-neighbor (NN) bonds (of strength $J_1 > 0$) competing with next-nearest-neighbor (NNN) bonds (of strength $J_2 \equiv \alpha J_1 > 0$). This quantum system has two different quasiclassical phases with collinear magnetic long-range order (LRO) at small ($\alpha < \alpha_{c_1} \approx 0.4$) and large ($\alpha > \alpha_{c_2} \approx 0.6$) values of the frustration strength parameter α , separated by an intermediate quantum paramagnetic phase with no magnetic LRO in the regime $\alpha_{c_1} < \alpha < \alpha_{c_2}$. Interest in this model has been greatly stimulated recently by its experimental realization in such layered magnetic materials as $\text{Li}_2\text{VO}\text{SiO}_4$,^{4,5} $\text{Li}_2\text{VO}\text{GeO}_4$,⁴ and VOMoO_4 .⁶ The syntheses of such layered quasi-2D materials has stirred up a great deal of renewed interest in the model (and see also, e.g., Refs. [7–10]). Amongst several methods that have been very successfully applied to the J_1 - J_2 model has been the coupled cluster method (CCM),^{11–14} which has also been applied to many similar strongly-interacting and highly frustrated spin-lattice models with comparable success. Other frustrated 2D models that have similarly engendered great recent interest include the spin- $\frac{1}{2}$ HAFs on the triangular^{15,16} and kagome lattices.^{17,18}

There has been a large amount of recent experimental investigation of the properties of quasi-2D magnetic materials with a ferromagnetic (FM) NN coupling ($J_1 < 0$) and an antiferromagnetic (AFM) NNN coupling ($J_2 > 0$). Examples include $\text{Pb}_2\text{VO}(\text{PO}_4)_2$,^{19–23}

(CuCl)LaNb₂O₇,²⁴ SrZnVO(PO₄)₂,^{22,25,26} BaCdVO(PO₄)₂,^{21,25,27} PbZnVO(PO₄)₂,²⁸ and (CuBr)LaNb₂O₇.²⁹ These experimental studies have also served to reignite interest in the theoretical investigation of the gs and thermodynamic properties of the FM J_1 - J_2 model, i.e., the model with FM NN exchange ($J_1 < 0$) and frustrating AFM NNN exchange ($J_2 > 0$).³⁰⁻⁴¹ Interestingly, arguments for the existence of a spin-nematic phase between two quasiclassical magnetically-ordered phases were presented.^{31,36,37,41} On the other hand, the existence of such a non-classical magnetically-disordered phase was also questioned in Ref. [39].

Other systems that have grown in importance in the last few years are various spin- $\frac{1}{2}$ magnetic models defined on the 2D honeycomb lattice. Several such systems have been both theoretically and experimentally studied⁴²⁻⁵¹ intensively, partly because of their special properties and partly due to the recent syntheses of various quasi-2D honeycomb-lattice materials. One reason for the theoretical interest in such models on the 2D honeycomb lattice is that a spin-liquid phase has been found for the exactly solvable Kitaev model,⁵² in which the spin- $\frac{1}{2}$ particles reside on just such a lattice. Furthermore, the honeycomb lattice is obviously germane to the very active research field of graphene, where the relevant physics may well be described by Hubbard-like models on this lattice.^{47,53,54} Interestingly, Meng *et al.*⁵⁴ found that for the Hubbard model on the honeycomb lattice with moderate values of the Coulomb repulsion parameter U , strong quantum fluctuations lead to an insulating spin-liquid phase between the non-magnetic metallic phase and the AFM Mott insulator phase. From the experimental side recent observations on the spin- $\frac{3}{2}$ honeycomb-lattice HAF Bi₃Mn₄O₁₂(NO₃) demonstrate a spin-liquid-like behavior at temperatures much lower than the Curie-Weiss temperature.⁵¹

We have recently studied⁵⁵ the AFM J_1 - J_2 - J_3 honeycomb model for the case where the spin quantum number s of each of the spins on every lattice site is $s = \frac{1}{2}$, and with AFM nearest-neighbor exchange bonds ($J_1 > 0$) in the presence of frustration caused by AFM NNN bonds ($J_2 > 0$) and with next-next-nearest neighbor (NNNN) bonds of strength J_3 also present, for the special case where $J_3 = J_2$. We found⁵⁵ that the scenario of deconfined criticality may hold for this model (and see also Ref. [48]). To date there exist only limited studies of the corresponding FM J_1 - J_2 - J_3 model (namely where $J_1 < 0$). In this paper, we further the investigation into the FM J_1 - J_2 - J_3 honeycomb model with FM NN bonds (of strength $J_1 < 0$) in the presence of frustrating AFM NNN bonds (of strength $J_2 > 0$) and NNNN bonds (of strength $J_3 > 0$). Once again we consider only the interesting

special case where $J_3 = J_2$. We focus our attention in the present study particularly on the detection and characterization of the gs phases of the quantum model. Bearing in mind the controversial discussion of the corresponding J_1 - J_2 square-lattice model with FM NN exchange bonds ($J_1 < 0$), the question naturally arises as to whether any indications for a non-classical magnetically-disordered phase might now be found for the honeycomb model. To determine the relevant gs phases and their properties we calculate the gs energy, the spin-spin correlation function, and the magnetic order parameter for the stripe-ordered state discussed below that is present as a gs phase in the corresponding classical version (equivalent to the $s \rightarrow \infty$ limit) of the model.

In view of its proven past ability to give results of high accuracy for a wide variety of highly frustrated 2D spin-lattice models, we again use the coupled cluster method (CCM) as our main computational tool in this paper. Additionally, we use the exact diagonalization (ED) method for a large finite lattice of $N = 32$ spins as a validity check of our CCM results. Since at the classical level the model now under consideration also exhibits some similarities with the corresponding model with AFM NN bonds ($J_1 > 0$), we compare our results for the quantum model of the FM case ($J_1 \equiv -1$) with those of the corresponding AFM case ($J_1 \equiv +1$).

The rest of the paper is organized as follows. After describing the model in Sec. II, we apply the CCM to investigate its gs properties. The CCM itself is very briefly described in Sec. III, before presenting and discussing our CCM and ED results in Sec. IV. We conclude in Sec. V with a summary of the main results.

II. THE MODEL

The Hamiltonian of the spin- $\frac{1}{2}$ J_1 - J_2 - J_3 Heisenberg model on the honeycomb lattice, which we studied recently⁵⁵ for the AFM case ($J_1 > 0$) is defined as

$$H = J_1 \sum_{\langle i,j \rangle} \mathbf{s}_i \cdot \mathbf{s}_j + J_2 \sum_{\langle\langle i,k \rangle\rangle} \mathbf{s}_i \cdot \mathbf{s}_k + J_3 \sum_{\langle\langle\langle i,l \rangle\rangle\rangle} \mathbf{s}_i \cdot \mathbf{s}_l, \quad (1)$$

where i runs over all lattice sites on the lattice, and where j runs over all NN sites connected to site i by J_1 bonds, k runs over all NNN sites connected to site i by J_2 bonds, and l runs over all NNNN sites connected to site i by J_3 bonds, but counting each bond once and once only in the three sums. Each site i of the lattice carries a spin- $\frac{1}{2}$ particle with spin operator

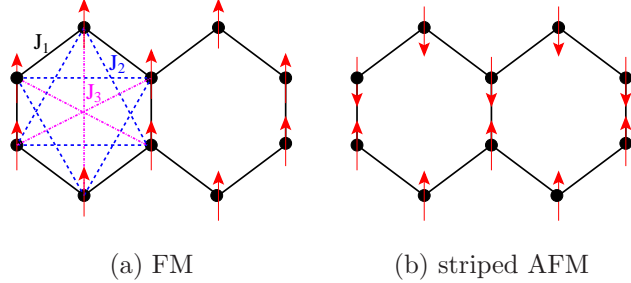


FIG. 1: (Color online) The J_1 - J_2 - J_3 honeycomb model, showing (a) the ferromagnetic (FM) state and (b) the classical striped antiferromagnetic (AFM) state. The arrows represent spins located on lattice sites \bullet .

$\mathbf{s}_i \equiv (s_i^x, s_i^y, s_i^z)$. We note that precisely the same model has also been studied recently on the square lattice, both in the case where all the bonds are AFM in nature,⁵⁶ and in the FM case where $J_1 < 0$ and $J_2 > 0, J_3 > 0$.⁵⁷

The aim of the present work is now to study further the spin- $\frac{1}{2}$ J_1 - J_2 - J_3 FM model (namely the above model in the case $J_1 < 0$) on the honeycomb lattice.^{43-46,58} The lattice and the exchange bonds are illustrated in Fig. 1(a). The classical gs phase diagram for the J_1 - J_2 - J_3 AFM model (with $J_1 > 0$) on the honeycomb lattice model displays collinear Néel and striped phases, both AFM in nature, as well as a spiral phase. These phases meet in a triple point at $J_3 = J_2 = J_1/2$ (and for more details see, e.g., Ref. [45]). For the remainder of this paper we again focus on the case where $J_3 = J_2 > 0$, but now where the NN exchange bond is FM in nature ($J_1 < 0$). The gs energies of the only two corresponding classical collinear states are then given by

$$\begin{aligned} \frac{E_{\text{FM}}^{\text{cl}}}{N} &= s^2 \left(\frac{3}{2}J_1 + \frac{9}{2}J_2 \right), \\ \frac{E_{\text{striped AFM}}^{\text{cl}}}{N} &= s^2 \left(\frac{1}{2}J_1 - \frac{5}{2}J_2 \right), \end{aligned} \quad (2)$$

for the FM state and collinear striped AFM state shown in Figs. 1(a) and (b) respectively. If these were the only gs phases in this $J_1 < 0$ regime we would thus have a classical transition between the FM state and the striped AFM state at $J_2^{\text{cl}} = -\frac{1}{7}J_1$ (≈ 0.143 for $J_1 = -1$) and a classical energy per site at this point of $E^{\text{cl}}/N = -\frac{3}{14} \approx -0.214$ for the $s = \frac{1}{2}$ system with $J_1 = -1$. For the corresponding AFM model with $J_1 > 0$ such a striped AFM state also exists as stated above, but the classical transition between the AFM Néel state and the striped AFM state is at $J_2 = +\frac{1}{2}J_1$. The reason why the corresponding phase transition in

the FM model occurs at a smaller value of the frustration parameter, $J_2^{\text{cl}}/|J_1| = \frac{1}{7}$ than the value $J_2^{\text{cl}}/J_1 = \frac{1}{2}$ for the AFM model is due to the $J_3(> 0)$ NNNN exchange bonds that act to frustrate the fully polarized FM state, whereas they reinforce the AFM Néel state. By contrast, the $J_2(> 0)$ NNN exchange bonds act to frustrate the J_1 bonds for both the FM state of the FM model and the Néel state of the AFM model. We note that the classical FM state is also an eigenstate of the Hamiltonian, with energy eigenvalue equal to the energy of its classical FM counterpart.

We note, however, that in fact the classical J_1 - J_2 - J_3 Heisenberg model on the honeycomb lattice with $J_1 < 0$, $J_2 > 0$, and $J_3 > 0$ also has a spiral phase that intervenes in a very narrow strip between the FM phase and the collinear striped AFM phase. (In Refs. [45,59] this is referred to as phase V.) The region in the x - y plane (where $x \equiv J_2/J_1$ and $y \equiv J_3/J_1$) in which it is the stable gs phase in the case $J_1 < 0$ is bounded by the three curves (i) $y = 0$, $-\frac{1}{2} < x < -\frac{1}{6}$, (ii) $y = -\frac{3}{2}x - \frac{1}{4}$, $-\frac{1}{6} < x < \frac{1}{2}$, and (iii) $y = \frac{1}{8}[1 - 6x - \sqrt{36x^2 + 20x + 17}]$, $-\frac{1}{2} < x < \frac{1}{2}$. The point $(x = \frac{1}{2}, y = -1)$ is a classical tetracritical point at which the spiral phase V meets the FM phase, the striped collinear AFM phase, and the AFM Néel phase (and see Fig. 3 of Ref. [45] for further details). Thus, in our case, where $J_3 = J_2$ and $J_1 < 0$, the classical spiral phase V exists in the narrow region $\frac{1}{10} < J_2/|J_1| < \frac{1}{5}$. Naturally this includes the point $J_2^{\text{cl}}/|J_1| = \frac{1}{7}$ discussed above at which the FM and striped collinear AFM phases would meet in the absence of the spiral phase V as a stable gs phase intervening between them.

In all of our results below for the FM J_1 - J_2 - J_3 honeycomb system we henceforth set $J_1 \equiv -1$ with no loss of generality, since this simply sets the overall scale of the Hamiltonian, and we consider the case where $J_3 = J_2 > 0$, such that both the NNN and NNNN bonds act to frustrate the ferromagnetism.

III. COUPLED CLUSTER METHOD

The CCM (see, e.g., Refs. [60–62] and references cited therein) that we use here is one of the most powerful and most versatile modern techniques in quantum many-body theory. It has been used to study various quantum magnets (see, e.g., Refs. [11–14,61–71] and references cited therein) very successfully. The method is particularly suitable for investigating frustrated systems, due to the fact that some of the main alternative methods are restricted

by certain problems that arise in such cases. For instance, quantum Monte Carlo (QMC) techniques suffer from the infamous and well-known “sign problem” for such systems. The exact ED method is also usually restricted by available computational power to relatively small finite-sized lattices. Nevertheless it can often be used, as here, to provide a handy tool to check and validate the results of other numerical or approximate methods.

We briefly describe here some of the important features of the CCM as applied to spin-lattice problems (and see, e.g., Refs. [11,61–65] and references cited therein for further details). The starting point for any CCM calculation is to select a normalized state $|\Phi\rangle$ as a reference or model state against which to incorporate in a systematic and potentially exact fashion the correlations present in the exact ground state. We often use a relevant classical ground state as the model state for spin systems for the sake of convenience, but other appropriate states may certainly also be used. In order to treat each site equivalently, a mathematical rotation of the local axes of the spins is conveniently performed in such a way that all spins in the reference state align along the same direction, say the negative z -axis. Clearly, such rotations leave unchanged the $SU(2)$ commutation relations between components of the spin operators.

The exact ket and bra gs energy eigenstates, $|\Psi\rangle$ and $\langle\tilde{\Psi}|$, of the many-body system are then parametrized in the CCM form as:

$$|\Psi\rangle = e^S|\Phi\rangle; \quad S = \sum_{I \neq 0} \mathcal{S}_I C_I^+, \quad (3)$$

$$\langle\tilde{\Psi}| = \langle\Phi|\tilde{\mathcal{S}}e^{-S}; \quad \tilde{\mathcal{S}} = 1 + \sum_{I \neq 0} \tilde{\mathcal{S}}_I C_I^-, \quad (4)$$

where

$$H|\Psi\rangle = E|\Psi\rangle; \quad \langle\tilde{\Psi}|H = E\langle\tilde{\Psi}|, \quad (5)$$

are the Schrödinger gs ket and bra equations respectively. The multiconfigurational creation operators $C_I^+ \equiv (C_I^-)^\dagger$ are defined so that $\langle\Phi|C_I^+ = 0 = C_I^-|\Phi\rangle; \forall I \neq 0$, and where we have defined $C_0^+ \equiv 1 \equiv C_0^-$. They are required to form a complete set of mutually commuting many-body creation operators in the Hilbert space, defined with respect to $|\Phi\rangle$ as a cyclic vector. Clearly the states are normalized such that $\langle\tilde{\Psi}|\Psi\rangle = \langle\Phi|\Psi\rangle = \langle\Phi|\Phi\rangle \equiv 1$. For spin-lattice systems they take the form of multi-spin raising operators and are written as products of single-spin raising operators, $C_I^+ \equiv s_{j_1}^+ s_{j_2}^+ \cdots s_{j_n}^+$, where $s_j^+ \equiv s_j^x + i s_j^y$. The

TABLE I: Number of fundamental LSUB m configurations (N_f) for the collinear striped AFM state of the spin- $\frac{1}{2}$ J_1 - J_2 - J_3 honeycomb model.

Method	N_f
LSUB6	72
LSUB8	941
LSUB10	14679
LSUB12	250891

gs energy is calculated in terms of the correlation coefficients $\{\mathcal{S}_I\}$ as $E = \langle \tilde{\Psi} | H | \Psi \rangle = \langle \Phi | e^{-S} H e^S | \Phi \rangle$; and the average on-site magnetization M in the rotated spin coordinates is calculated equivalently in terms of the coefficients $\{\mathcal{S}_I, \tilde{\mathcal{S}}_I\}$ as $M \equiv -\frac{1}{N} \langle \tilde{\Psi} | \sum_{j=1}^N s_j^z | \Psi \rangle$, which now plays the role of the order parameter. Finally, the complete set of unknown ket- and bra-state correlation coefficients $\{\mathcal{S}_I, \tilde{\mathcal{S}}_I\}$ is calculated by requiring the expectation value $\bar{H} = \langle \tilde{\Psi} | H | \Psi \rangle$ to be a minimum with respect to all parameters $\{\mathcal{S}_I, \tilde{\mathcal{S}}_I ; \forall I \neq 0\}$. This readily leads to the coupled set of nonlinear equations for the ket-state creation correlation operators $\{\mathcal{S}_I\}$, $\langle \Phi | C_I^- e^{-S} H e^S | \Phi \rangle = 0 ; \forall I \neq 0$, and to the coupled set of linear equations, $\langle \Phi | \tilde{\mathcal{S}}_I (e^{-S} H e^S - E) C_I^+ | \Phi \rangle = 0 ; \forall I \neq 0$, which can then be solved for the bra-state destruction correlation operators $\{\tilde{\mathcal{S}}_I\}$.

When all many-body configurations $\{I\}$ are included in the expansions of the correlation expansions operators S and \tilde{S} , the CCM formalism is exact. However, it is necessary of course in practice to use approximation schemes to truncate the sets of configurations $\{I\}$ contained in the expansions of Eqs. (3) and (4) for the CCM correlation operators. For systems defined on a regular periodic spatial lattice as here, it is convenient to use the well-established LSUB m approximation scheme in which all possible multi-spin-flip correlations over different locales on the (here, honeycomb) lattice defined by m or few contiguous lattice sites are retained. Clusters are defined to be contiguous in this sense if every site in the cluster is adjacent (as a nearest neighbor) to at least one other site in the cluster. This is the scheme we use for all our results presented below. The number N_f of independent fundamental clusters (i.e., those that are inequivalent under the symmetries of the Hamiltonian and of the model state) increases rapidly with the truncation index m , as shown in Table I for the present spin- $\frac{1}{2}$ J_1 - J_2 - J_3 model on the honeycomb lattice, where we use the natural

lattice geometry itself to define the notion of adjacency inherent in the definition of the LSUB m scheme. We see, for example, that the number N_f of such fundamental clusters (and hence the number of simultaneous nonlinear equations we need to solve for the retained correlation coefficients $\{\mathcal{S}_I\}$) for the striped model state is 250891 at the highest LSUB12 level of approximation that we utilize here. The corresponding numbers, N_f , of fundamental configurations are appreciably higher at a given LSUB m level when the spiral phase V is used as the CCM model state, due to the considerably reduced symmetry. It is necessary to use massive parallelization and supercomputing resources in order to perform the CCM calculations at such high level of approximation.⁷² Thus, for example, to obtain a single data point (i.e., for a given value of $J_3 = J_2$) for the striped model state at the LSUB12 level typically requires about 0.5 h computing time using 1000 processors simultaneously.

We present CCM results below based on the striped collinear AFM state as model state, at various LSUB m levels of approximation with $m = \{6, 8, 10, 12\}$, and also in the corresponding $m \rightarrow \infty$ extrapolated limits (LSUB ∞) based on the well-tested extrapolation schemes described below and in more detail elsewhere.^{11–13,61,62} We have also performed extrapolations for the data set with $m = \{6, 8, 10\}$. Both sets of results agree well with one another, which gives added credence to our results. Note that we do not use the LSUB m approximation scheme for values $m < 6$ of the truncation index, since these low-order approximations will not capture the natural hexagonal structure of the lattice. We remark that, as always, the CCM exactly obeys the Goldstone linked-cluster theorem at every LSUB m level of approximation. Hence we work from the outset in the limit $N \rightarrow \infty$, where N is the number of sites on the honeycomb lattice, and extensive quantities such as the gs energy are always guaranteed to be linearly proportional to N in this limit.

We clearly do not need to perform any finite-size scaling of our results, as all CCM approximations are automatically performed from the outset in the infinite-lattice limit, $N \rightarrow \infty$, as discussed above. It is, however, necessary to extrapolate to the exact $m \rightarrow \infty$ limit in the LSUB m truncation index m , in which limit the complete (infinite) Hilbert space is reached. For the gs energy per spin, E/N , a well-tested and very accurate extrapolation ansatz (and see, e.g., Refs., [12,13,39,64,73,74]) is

$$E(m)/N = a_0 + a_1 m^{-2} + a_2 m^{-4}, \quad (6)$$

while for the magnetic order parameter, M , different schemes have been employed for dif-

ferent situations. For models showing no or only relatively small amounts of frustration, a well-tested and accurate rule (and see, e.g., Refs. [64,73]) is

$$M(m) = b_0 + b_1 m^{-1} + b_2 m^{-2}. \quad (7)$$

For highly frustrated systems, particularly those showing a gs order-disorder transition, a more appropriate extrapolation rule with fixed exponents that has been found to give good results (and see, e.g., Refs. [12,39]) is

$$M(m) = c_0 + c_1 m^{-1/2} + b_2 m^{-3/2}. \quad (8)$$

We give illustrations here of the use of each of these schemes, wherever and whenever possible.

IV. RESULTS AND DISCUSSION

We now present and discuss our CCM results. In order to have an independent check on the accuracy and consistency of our CCM results, we have also performed additional computations of selected gs properties of the present models using the ED technique that is a well-established and successful tool for studying frustrated quantum spin systems (and see, e.g., Refs. [39,48,75–78]). In Fig. 2(a) we show the CCM results for the gs energy per spin, E/N , in various LSUB m approximations based on the striped state as CCM model state, as well as the exact gs energy for a finite lattice of size $N = 32$. We also show separately, in Fig. 2(b), the extrapolated ($m \rightarrow \infty$) results obtained from Eq. (6) using the data set $m = \{6, 8, 10, 12\}$. Comparison is made with the results for the corresponding AFM version of the model with $J_1 = +1$.

The CCM LSUB m data displayed in Fig. 2(a) show that the gs energy results converge extremely rapidly as the truncation index m is increased, such that the difference between the LSUB12 results and the extrapolated ($m \rightarrow \infty$) results obtained from Eq. (6) is very small indeed. We note too that, just as in the corresponding AFM case of the model with $J_1 = +1$, the various CCM LSUB m solutions based on the striped model state now also terminate at some lower termination point J_2^t as J_2 is decreased. Such terminations of CCM solutions are very common and have been very well documented.⁶² In all such cases a termination point always arises due to the solution of the CCM equations becoming

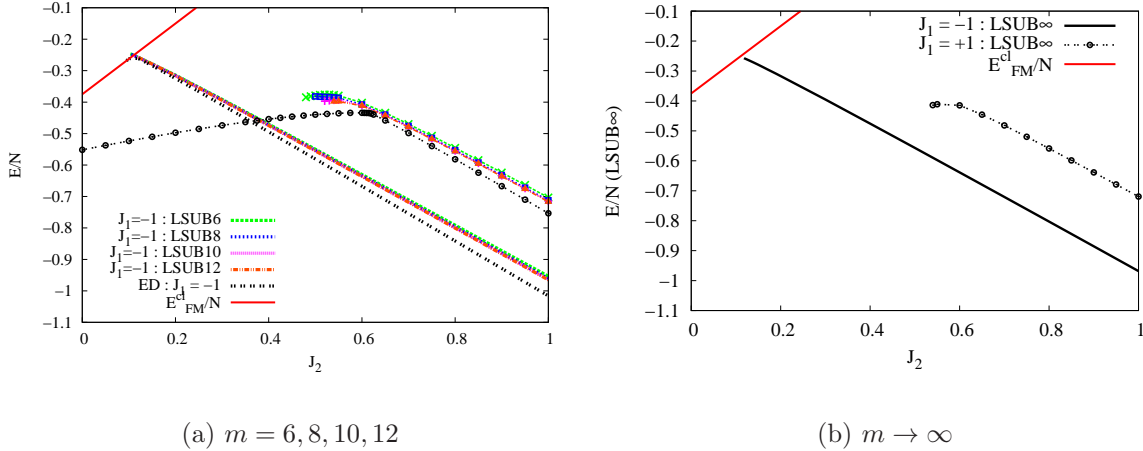


FIG. 2: (Color online) Ground-state energy per spin, E/N , versus J_2 for the striped phase of the spin- $\frac{1}{2}$ J_1 - J_2 - J_3 honeycomb model with $J_1 = -1$ compared with those for $J_1 = +1$ (with $J_3 = J_2 > 0$ for both cases). The CCM results using the striped model state for various LSUB m approximations with $m = \{6, 8, 10, 12\}$, together with the ED ($N = 32$) results are shown in (a). We show in (b) the extrapolated CCM LSUB ∞ results using the $m = \{6, 8, 10, 12\}$ data points fitted to Eq. (6). In all cases curves without symbols attached refer to the case $J_1 = -1$, whereas the corresponding curves with symbols refer to the case $J_1 = +1$. The FM result from Eq. (2) with $s = \frac{1}{2}$ is also displayed.

complex at this point, beyond which there exist two branches of entirely unphysical complex conjugate solutions.⁶² In the region where the solution reflecting the true physical solution is real there actually also exists another (unstable) real solution. However, only the shown branch of these two solutions reflects the true (stable) physical ground state, whereas the other branch does not. The physical branch is usually easily identified in practice as the one which becomes exact in some known (e.g., perturbative) limit. This physical branch then meets the corresponding unphysical branch at some termination point with infinite slope, beyond which no real solutions exist. The LSUB m termination points are themselves also reflections of the quantum phase transitions in the real system and may be used to estimate the position of the phase boundary,⁶² although we do not do so for this critical point in the FM model, since we have more accurate criteria that we now discuss.

We note first from Fig. 2(a) that the LSUB m termination points using the striped state as the CCM model state for the present FM version of the model with $J_1 = -1$, lie very

close indeed to the points where the curves cross (or nearly cross) the corresponding curve for the FM state given by Eq. (2). This gives us our first evidence that either there is no intermediate phase between the quantum striped phase and the FM phase for the case $J_1 = -1$, or, if one exists, it can occur only over a very narrow regime indeed. This situation may be contrasted with that of the AFM version of the model ($J_1 = +1$),⁵⁵ where the LSUB m results for the gs energy using the striped model state terminate before they meet the corresponding results using the Néel state as model state (which themselves also terminated at some upper termination points that were lower in value than the lower termination points for the striped state). In the latter case there is an intermediate plaquette valence-bond crystal (PVBC) phase.

At the classical level the difference in the values of the gs energy per spin of the collinear striped states between the two $s = \frac{1}{2}$ cases (i.e., for positive and negative values of J_1 with $|J_1| = 1$) is 0.25, independent of J_2 and J_3 . The quantum versions follow this pattern for larger values of $J_3 = J_2$, as seen from Fig. 2, but the constancy in the difference breaks down at around $J_2 \approx 0.6$, where the AFM case ($J_1 = +1$) exhibits a critical point marking a transition to the PVBC phase, which then in turn undergoes a further phase transition to the Néel phase at another lower critical value. The corresponding best available CCM estimates for those two critical values for the AFM case of the model with $J_1 = +1$ are $J_2^{c2} \approx 0.60$ and $J_2^{c1} \approx 0.47$ respectively.⁵⁵ In the present FM case of the model with $J_1 = -1$ we see no evidence (apart from the seeming termination of the solutions to the equations for the LSUB12 approximation based on the striped state as CCM model state very slightly before the gs energy crossing point with the FM state) of any similar intermediate state between the FM state and the collinear striped AFM state. If any such intermediate state exists at all, however, it must be confined to a very narrow region indeed around $J_2 \approx 0.11$, probably confined to $0.10 \lesssim J_2 \lesssim 0.12$. We return to a more detailed discussion of this region later. For the moment we note only that it is much reduced from the region $0.1 < J_2 < 0.2$ in which the corresponding classical version of the model has the spiral phase V as its stable gs phase.

For the present FM case with $J_1 = -1$ the CCM LSUB m gs energy curves using the striped model state cross the corresponding gs energy curve for the FM state from Eq. (2) for $m = \{6, 8, 10\}$ at corresponding critical values $J_2^c(\text{LSUB6}) \approx 0.1106$ (where $E_{\text{LSUB6}}^c/N \approx -0.2506$), $J_2^c(\text{LSUB8}) \approx 0.1101$ (where $E_{\text{LSUB8}}^c/N \approx -0.2511$), and $J_2^c(\text{LSUB10}) \approx 0.1098$

(where $E_{\text{LSUB10}}^c/N \approx -0.2515$). The corresponding LSUB12 result for the gs energy using the striped state as the CCM model state appears to terminate just before meeting the gs energy curve for the FM phase. However we note that for such very high-order CCM calculations it becomes very computationally expensive to determine the termination point with high accuracy. If we use the extrapolated LSUB ∞ results for the gs energy for the striped phase by making use of Eq. (6) and employing the whole data set $m = \{6, 8, 10, 12\}$, we thus need to perform a further very small extrapolation of the CCM results to lower values of J_2 to find the presumed crossing point of the energies of the striped and FM phases, in the scenario in which these two phases meet at a first-order transition with no intermediate phase (that would itself be confined to the very narrow intervening region $0.10 \lesssim J_2 \lesssim 0.12$, as discussed above). As expected, simple power-law expansions give very accurate fits, and give crossing points very close to those above. Putting all the energy data together, our best estimate for the critical point of the first-order phase transition from the collinear striped phase to the FM phase (in the scenario where this transition occurs directly, with no intermediate phase confined to the narrow region $0.10 \lesssim J_2 \lesssim 0.12$) for the spin- $\frac{1}{2}$ J_1 - J_2 - J_3 Heisenberg ferromagnet (with $J_1 = -1$) on the honeycomb lattice, and with $J_3 = J_2 > 0$, is $J_2^c = 0.1095 \pm 0.0005$, at which point the gs energy per spin is $E^c/N = -0.2518 \pm 0.0006$.

We see from Fig. 2(a) that the agreement between the ED ($N = 32$) and the CCM energies is very satisfactory. Moreover, due to the finite-size scaling of the gs energy, $E/N = e_0 - a/N^{3/2}$ with $a > 0$ (and see, e.g. Refs. [75] and [77]), the difference between the CCM and the ED gs energies would become even smaller if finite lattices of larger size could be considered. The ED turnover point in the energy curve that marks the termination of the FM phase occurs at a value of about 0.1003 for the $N = 32$ lattice used, and for the same reasons as above this value will increase as N is increased. Thus, in summary, while the CCM estimates for the gs energy per spin for the spin- $\frac{1}{2}$ J_1 - J_2 - J_3 Heisenberg model on the extended infinite honeycomb lattice are much more accurate than the ED results, the latter do serve as an independent check on the former.

The hypothetical phase transition (i.e., when the existence of the intervening spiral phase V is momentarily ignored) from FM order to collinear striped AFM order for the classical version of the FM model with $J_1 = -1$ occurs at a value $J_2^{\text{cl}} = \frac{1}{7} \approx 0.143$, compared with the corresponding value $J_2^c \approx 0.110$ found here. Thus quantum fluctuations act to stabilize the collinear AFM order, at the expense of the FM order, to higher values of frustration

than in the classical case. It is interesting to note that a similar situation was found in the FM version ($J_1 = -1, J_2 > 0$) of the spin- $\frac{1}{2}$ J_1 - J_2 model on the square lattice,³⁹ where a quantum critical point exists at a value $J_2^c \approx 0.39$ for a similar transition from FM order to collinear striped order, compared with a corresponding classical value of $J_2^{\text{cl}} = 0.5$. It is well known, from many cases studied, that quantum fluctuations almost always favor collinear states over noncollinear ones (e.g., spiral or canted states). What is interesting in both the present case and the spin- $\frac{1}{2}$ J_1 - J_2 model on the square lattice cited above, is that quantum fluctuations seem also to favor one collinear state (namely the collinear striped AFM state in these two cases) where the quantum fluctuations are present, over another collinear state (namely the FM state in these two cases) where quantum fluctuations are absent. It is intriguing to wonder whether these are examples of a more general rule.

We present results in Fig. 3 for the CCM collinear stripe order parameter M , as defined in Sec. III. Figure 3(a) shows LSUB m results with $m = \{6, 8, 10, 12\}$, while Fig. 3(b) shows the corresponding extrapolated CCM LSUB ∞ ($m \rightarrow \infty$) results using both Eqs. (7) and (8). We note firstly that the CCM LSUB m order parameter results depend on the approximation level m much more strongly than those for the gs energy. It is clear that the order parameter behaves similarly for large values of J_2 for both the FM model ($J_1 < 0$) and the AFM model ($J_1 > 0$). However, once again there are considerable differences in the behavior of M between the two models for values of the frustration parameter $J_2/|J_1| \lesssim 0.6$. The extrapolated CCM results for M for the AFM model in Fig. 3(b) clearly show the breakdown of the quasiclassical collinear magnetic LRO near the critical value of $J_2 \approx 0.6$, i.e., significantly above the classical transition point $J_2^{\text{cl}} = 0.5$ (and see, e.g., Refs. [44,48,49,55]). Indeed, the CCM estimate for the critical value of the frustration parameter in the AFM case for the disappearance of collinear striped order is $J_2^{c2} \approx 0.60$ from the point at which M becomes zero, using the extrapolation scheme of Eq. (8).⁵⁵ By contrast, the order parameter for the FM model stays almost constant over the whole parameter region shown in Fig. 3. We do not observe any indication of the breakdown of the collinear striped magnetic LRO until $J_2 \approx 0.11$ for the FM model, which is below the hypothetical classical transition point $J_2^c \approx 0.143$, as we observed previously in the results for the gs energy.

Lastly, we present results for various spin-spin correlation functions for the FM as well as for the AFM model in Fig. 4. Figure 4(a) shows the CCM LSUB10 results and Fig. 4(b) shows the corresponding ED results. Once again we note that for large values of the frus-

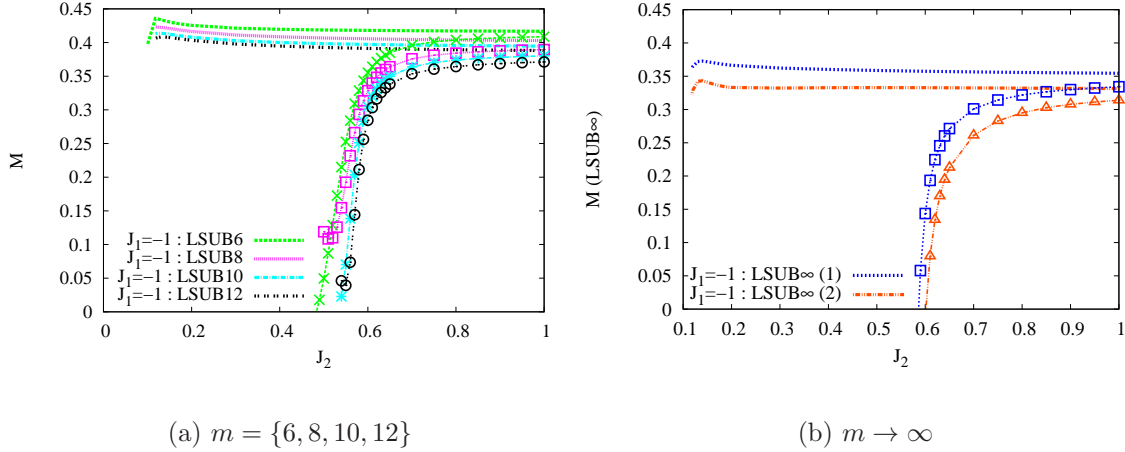


FIG. 3: (Color online) Ground-state magnetic order parameter, M , for the striped AFM state of the spin- $\frac{1}{2}$ J_1 - J_2 - J_3 honeycomb model with $J_1 = -1$, compared with those for $J_1 = +1$ (with $J_3 = J_2 > 0$ for both cases). The CCM results for various LSUB m approximations with $m = \{6, 8, 10, 12\}$ are shown in (a). We also show in (b) the extrapolated LSUB ∞ results using the $m = \{6, 8, 10, 12\}$ data points. The curves labelled LSUB ∞ (1) and LSUB ∞ (2) are obtained using Eq. (7) and Eq. (8) respectively. In all cases curves without symbols attached refer to the case $J_1 = -1$, whereas the corresponding curves with symbols refer to the case $J_1 = +1$.

tration parameter J_2 the corresponding spin-spin correlations functions for both the FM ($J_1 = -1$) and AFM ($J_1 = +1$) models agree remarkably well with one another for both the CCM and ED calculations. Furthermore, for the FM model the agreement of the CCM correlation functions with the ED data is excellent. For the AFM model the agreement between the CCM and ED results is again excellent for values of J_2 above the transition point at which the AFM collinear striped order disappears, namely $J_2^{c2} \approx 0.60$, but around and below this value there are noticeable differences. In particular, the very steep change in the correlation functions at $J_2 \approx 0.62$ present in the ED ($N = 32$) data for the AFM model is not observed in the CCM LSUB10 data. Instead the CCM data show a smoother change in that region. However, we have argued⁵⁵ that for $J < J_2^{c2} \approx 0.60$ no striped magnetic LRO order exists. Indeed we argued that no magnetic LRO order exists at all for the AFM model in the regime $J_2^{c1} < J < J_2^{c2}$, where instead we have a PVBC state. Hence, it is not surprising that the CCM solution in a finite order of LSUB m approximation based on

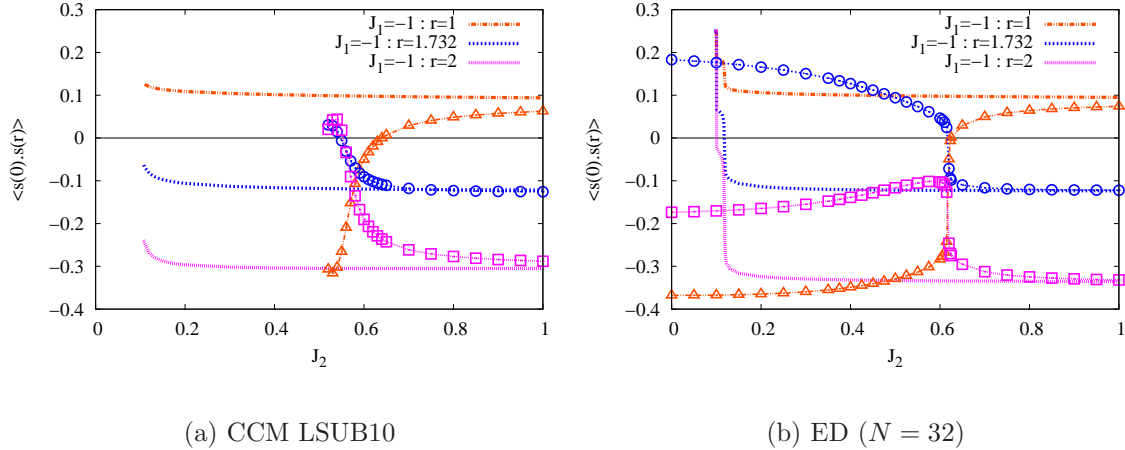


FIG. 4: (Color online) Selected spin-spin correlation functions $\langle \mathbf{s}(0) \cdot \mathbf{s}(\mathbf{r}) \rangle$ for the spin- $\frac{1}{2}$ J_1 - J_2 - J_3 model on the honeycomb lattice with $J_3 = J_2$, for both the FM case (with $J_1 = -1$) and the AFM case (with $J_1 = +1$), using (a) the CCM with the striped collinear state as model state, at the LSUB10 level of approximation; and (b) the ED method on a lattice of size $N = 32$. Values $r = 1, 1.732$ and 2 correspond respectively to NN, NNN, and NNNN pairs of spins. In all cases curves without symbols attached refer to the case $J_1 = -1$, whereas the corresponding curves with symbols refer to the case $J_1 = +1$.

the collinear stripe reference state does not provide such accurate results for the correlation functions inside this magnetically disordered phase.

To conclude, we return to examine more closely the very narrow region $0.10 \lesssim J_2 \lesssim 0.12$ for which our CCM results based on the striped AFM state as model state could not exclude the possibility of an intervening phase between the striped AFM and the FM phases. In Fig. 5 we show a more detailed view of the ED results for the same spin-spin correlation functions shown in Fig. 4(b) in this narrow region just above the FM transition point. The ED data does definitely indicate the existence of a phase in precisely the region $0.10 \lesssim J_2 \lesssim 0.12$. It is difficult from this data to say with any certainty whether or not the state is the quantum-mechanical remnant of the classical spiral phase V that exists in the classical regime $0.1 < J_2 < 0.2$. Furthermore, without ED calculations on larger lattices, for which the computational cost would be prohibitive, it is also not possible to say whether these results over such a narrow region are an artefact of the finite lattice size. Our results are summarized in Sec. V.

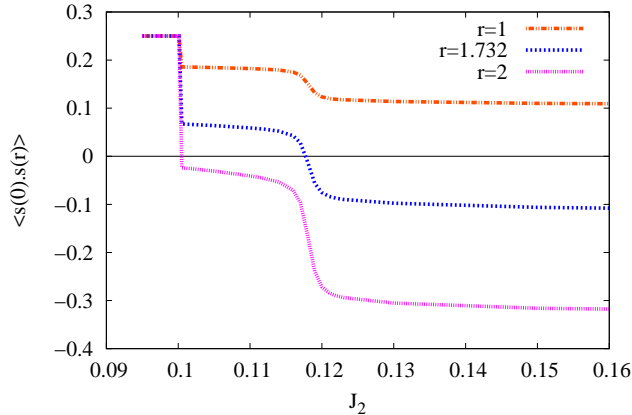


FIG. 5: (Color online) An expanded view near the FM boundary of the same spin-spin correlation functions $\langle \mathbf{s}(0) \cdot \mathbf{s}(\mathbf{r}) \rangle$ shown in Fig. 4(b) for the spin- $\frac{1}{2}$ J_1 - J_2 - J_3 model on the honeycomb lattice for the FM case with $J_1 = -1$ and $J_3 = J_2$ using the ED method on a lattice of size $N = 32$.

V. SUMMARY AND CONCLUSIONS

In this paper we have presented results on the gs properties of the spin- $\frac{1}{2}$ J_1 - J_2 - J_3 Heisenberg model with FM NN ($J_1 = -1$) exchange bonds in the presence of frustrating AFM NNN ($J_2 > 0$) and NNNN ($J_3 > 0$) exchange bonds of equal strength ($J_3 = J_2$) on the honeycomb lattice, using both the CCM and Lanczos ED. By comparison with previous studies for the AFM ($J_1 = +1$) version of the model,⁵⁵ we find similar behavior for both models for values $J_2 \gtrsim 0.6|J_1|$, but for values of $J_2 \lesssim 0.6|J_1|$ the models differ markedly. The results of the present paper for the FM version of the model and that of the previous paper⁵⁵ for the AFM version may conveniently be combined and summarised in the phase diagram shown in Fig. 6.

We note that, by contrast with the corresponding model with AFM NN exchange ($J_1 = +1$) we do not find indications for a non-classical magnetically-disordered phase for the model with FM NN exchange ($J_1 = -1$). If such a phase exists at all it must be confined to a very small range of the frustration parameter around $0.10 \lesssim J_2 \lesssim 0.12$. However, any such phase is much more likely to be a quasiclassical remnant of the spiral phase V that exists in the corresponding classical model (with $J_1 = -1$) in the parameter regime $0.1 < J_2 < 0.2$. As expected, quantum fluctuations then usually favor a collinear phase over a noncollinear

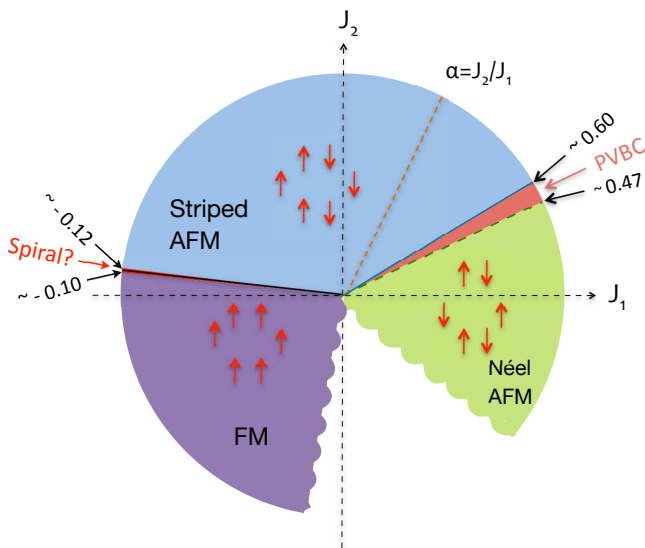


FIG. 6: (Color online) The phase diagram of the spin- $\frac{1}{2}$ J_1 - J_2 - J_3 honeycomb model in the J_1 - J_2 plane, for the case $J_3 = J_2$. The continuous transition between the AFM Néel and PVBC phases at $J_2/J_1 \approx 0.47$ is shown by a broken line, while the first-order transition between the PVBC and AFM striped phases at $J_2/J_1 \approx 0.60$ is shown by a solid line. Our results indicate that the transition between the striped AFM and FM phases is either a first-order one at $J_2/J_1 \approx -0.11$ or occurs via an intermediate phase, probably with noncollinear spiral order, which exists in the region $-0.12 \lesssim J_2/J_1 \lesssim 0.10$. The region between the FM and AFM Néel phases with $J_3 = J_2 < 0$ has not been investigated by us.

one, and the extent of any spiral phase is smaller in the quantum spin- $\frac{1}{2}$ case than in the classical ($s \rightarrow 0$) case.

In one scenario the results presented here for the case $J_1 = -1$ indicate a direct first-order transition between the two magnetically ordered phases, namely the FM ground state at small values of the frustration parameter J_2 and the striped collinear AFM ground state at larger values of J_2 . Our best estimate of the phase transition point is then $J_2^c = 0.1095 \pm 0.0005$. Although in this scenario a quasiclassical gs phase (viz., the collinear striped AFM state) exists in the whole parameter space down to the FM gs phase, the frustration might still have a strong effect on the low-temperature thermodynamics near the transition point at $J_2^c = 0.1095 \pm 0.0005$.^{38,39} For values $J_2 \gtrsim J_2^c$ the FM multiplet becomes a low-lying

excitation, and this might lead to an additional low-temperature peak in the specific heat $C(T)$.^{30,79,80} We note that indications for such an additional low-temperature peak in $C(T)$ were also found on the FM side near such a transition^{38,81} (i.e., at $J_2 \lesssim J_2^c$) in other frustrated spin models.

In an alternative scenario our results also indicate the possibility of an intervening phase between the collinear FM and striped AFM phases. Any such phase, however, is limited to lie within the very narrow range $0.10 \lesssim J_2 \lesssim 0.12$, as shown in Fig. 6. In principle we could more accurately establish the existence of such a phase as a quasiclassical remnant of the classical spiral phase V, and thence also more accurately establish its phase boundaries, by performing another comparable set of CCM calculations to those performed here with the striped AFM state as model state, but using instead the spiral state V as model state. Such calculations would be much more onerous and computationally expensive, however, since on the one hand the number N_f of fundamental CCM configurations at a given LSUB m level is greater for the spiral model state than for the striped model state and, furthermore, the CCM results would need to be optimized at a given LSUB m level with respect to the spiral pitch angle parameters by minimizing the corresponding result for the energy per spin separately for each set of values for the bond strength parameters.

We note finally that we have not yet investigated the present model in the case where $J_3 = J_2 < 0$. For the FM version of the model when $J_1 < 0$ also, the FM phase is then obviously the stable ground state. Conversely, when $J_1 > 0$ and frustration occurs, there is a direct first-order transition in the classical version of the model between the FM and Néel AFM states at a value $J_2/J_1 = -1$. Following the discussion in Sec. IV we might expect that quantum fluctuations could again act either (a) to retain the direct transition but to stabilize the collinear AFM order in preference to the FM order, thus pushing the phase boundary to a somewhat lower value, $J_2/J_1 < -1$, for the spin- $\frac{1}{2}$ case; or (b) to permit an intervening state with no classical counterpart. Indeed, very preliminary CCM calculations indicate that scenario (a) is realized and that this corresponding critical point may be pushed to a value $J_2/J_1 \approx -1.15 \pm 0.05$. We hope to report in more detail on this region and to give a more accurate value of this phase boundary in a future paper.

As discussed briefly in Sec. I, it has been proposed^{31,36,37,41} that the competition between FM Heisenberg interactions between NN pairs of spins and AFM interactions between other spins in frustrated spin- $\frac{1}{2}$ systems on the square lattice could lead to gapless spin-liquid

states with multipolar order (e.g., spin-nematic states) adjacent to the FM state. Similar states have also been proposed to arise in frustrated multiple cyclic spin-exchange models on the triangular lattice with FM NN pairwise interactions,⁸² either in the presence of a magnetic field (where octupolar order occurs) or in its absence (where quadratic or nematic ordering occurs in a state bordering the FM state). In the case of the frustrated honeycomb-lattice ferromagnet considered here we have found no evidence for such states. However, the multipolar-ordering phenomenon in the zero-field case considered here is evidently rather fragile, and in the square-lattice case for the spin- $\frac{1}{2}$ FM version of the J_1 - J_2 model (i.e., with $J_1 < 0$) even their existence has been questioned in recent rather accurate work³⁹ that also employed both high-order CCM and ED techniques. No evidence was found for such states either in a very recent Schwinger boson study on the square lattice,⁵⁷ using the same FM version of the spin- $\frac{1}{2}$ J_1 - J_2 - J_3 Heisenberg model that we studied here on the honeycomb lattice. Nevertheless, the history of the study of quantum magnets has shown us that the detection of phases with novel quantum ordering, such as nematic states of various kinds, is extremely subtle. In particular, the present honeycomb-lattice model surely warrants further investigation before the absence of nematic states in the FM case discussed here is considered definite.

Finally we mention that frustrated ferromagnets are also interesting with respect to multi-magnon bound states appearing in high magnetic fields (and see, e.g., Refs. [31,83–85]). The present model also warrants further investigation when the coupling to an external magnetic field is included.

ACKNOWLEDGMENTS

We thank the University of Minnesota Supercomputing Institute for Digital Simulation and Advanced Computation for the grant of supercomputing facilities, on which we relied for the numerical calculations reported here. One of the authors (DJJF) acknowledges and thanks the European Science Foundation for financial support under the research network

program “Highly Frustrated Magnetism” (short visit grant number 3858).

- ¹ U. Schollwöck, J. Richter, D. J. J. Farnell, and R. F. Bishop (eds.), *Quantum Magnetism*, Lecture Notes in Physics **645** (Springer-Verlag, Berlin, 2004).
- ² G. Misguich and C. Lhuillier, in *Frustrated Spin Systems*, edited by H.T. Diep (World Scientific, Singapore, 2005), p. 229.
- ³ J. B. Parkinson and D. J. J. Farnell, in *An Introduction to Quantum Spin Systems*, Chapter 11 Lecture Notes in Physics **816** (Springer-Verlag, Berlin, 2010).
- ⁴ R. Melzi, P. Carretta, A. Lascialfari, M. Mambrini, M. Troyer, P. Millet, and F. Mila, *Phys. Rev. Lett.* **85**, 1318 (2000).
- ⁵ H. Rosner, R. R. P. Singh, W. H. Zheng, J. Oitmaa, S.-L. Drechsler, and W. E. Pickett, *Phys. Rev. Lett.* **88**, 186405 (2002).
- ⁶ A. Bombardi, L. C. Chapon, I. Margiolaki, C. Mazzoli, S. Gonthier, F. Duc, and P. G. Radaelli, *Phys. Rev. B* **71**, 220406(R) (2005).
- ⁷ L. Capriotti and S. Sorella, *Phys. Rev. Lett.* **84**, 3173 (2000).
- ⁸ L. Capriotti, F. Becca, A. Parola, and S. Sorella, *Phys. Rev. Lett.* **87**, 097201 (2001).
- ⁹ R. R. P. Singh, W. Zheng, J. Oitmaa, O. P. Sushkov, and C. J. Hamer, *Phys. Rev. Lett.* **91**, 017201 (2003).
- ¹⁰ T. Roscilde, A. Feiguin, A. L. Chernyshev, S. Liu, and S. Haas, *Phys. Rev. Lett.* **93**, 017203 (2004).
- ¹¹ R. F. Bishop, D. J. J. Farnell, and J. B. Parkinson, *Phys. Rev. B* **58**, 6394 (1998).
- ¹² R. F. Bishop, P. H. Y. Li, R. Darradi, J. Schulenburg, and J. Richter, *Phys. Rev. B* **78**, 054412 (2008).
- ¹³ R. F. Bishop, P. H. Y. Li, R. Darradi, and J. Richter, *J. Phys.: Condens. Matter* **20**, 255251 (2008).
- ¹⁴ R. Darradi, O. Derzhko, R. Zinke, J. Schulenburg, S. E. Krüger, and J. Richter, *Phys. Rev. B* **78**, 214415 (2008).
- ¹⁵ B. Bernu, C. Lhuillier, and L. Pierre, *Phys. Rev. Lett.* **69**, 2590 (1992).
- ¹⁶ C. Zeng, I. Staples, and R. F. Bishop, *J. Phys.: Condens. Matter* **7**, 9021 (1995).
- ¹⁷ A. P. Schnyder, O. A. Starykh, and L. Balents, *Phys. Rev. B* **78**, 174420 (2008).

- ¹⁸ G. Evenbly and G. Vidal, Phys. Rev. Lett. **104**, 187203 (2010).
- ¹⁹ E. E. Kaul, H. Rosner, N. Shannon, R. V. Shpanchenko, and C. Geibel, J. Magn. Magn. Mater. **272-276**, 922 (2004).
- ²⁰ M. Skoulatos, J. P. Goff, N. Shannon, E. E. Kaul, C. Geibel, A. P. Murani, M. Enderle, and A. R. Wildes, J. Magn. Magn. Mater. **310**, 1257 (2007).
- ²¹ P. Carretta, M. Filibian, R. Nath, C. Geibel, and P. J. C. King, Phys. Rev. B **79**, 224432 (2009).
- ²² M. Skoulatos, J. P. Goff, C. Geibel, E. E. Kaul, R. Nath, N. Shannon, B. Schmidt, A. P. Murani, P. P. Deen, M. Enderle, and A. R. Wildes, Europhys. Lett. **88**, 57005 (2009).
- ²³ R. Nath, Y. Furukawa, F. Borsa, E. E. Kaul, M. Baenitz, C. Geibel, and D. C. Johnston, Phys. Rev. B **80**, 214430 (2009).
- ²⁴ H. Kageyama, T. Kitano, N. Oba, M. Nishi, S. Nagai, K. Hirota, L. Viciu, J. B. Wiley, J. Yasuda, Y. Baba, Y. Ajiro, and K. Yoshimura, J. Phys. Soc. Jpn. **74**, 1702 (2005).
- ²⁵ A. A. Tsirlin and H. Rosner, Phys. Rev. B **79**, 214417 (2009).
- ²⁶ A. A. Tsirlin, B. Schmidt, Y. Skourski, R. Nath, C. Geibel, and H. Rosner, Phys. Rev. B **80**, 132407 (2009).
- ²⁷ R. Nath, A. A. Tsirlin, H. Rosner, and C. Geibel, Phys. Rev. B **78**, 064422 (2008).
- ²⁸ A. A. Tsirlin, R. Nath, A. M. Abakumov, R. V. Shpanchenko, C. Geibel, and H. Rosner, Phys. Rev. B **81**, 174424 (2010).
- ²⁹ N. Oba, H. Kageyama, T. Kitano, J. Yasuda, Y. Baba, M. Nishi, K. Hirota, Y. Narumi, M. Hagiwara, K. Kindo, T. Saito, Y. Ajiro and K. Yoshimura, J. Phys. Soc. Jpn. **75**, 113601 (2006).
- ³⁰ N. Shannon, B. Schmidt, K. Penc, and P. Thalmeier, Eur. Phys. J. B **38**, 599 (2004).
- ³¹ N. Shannon, T. Momoi, and P. Sindzingre, Phys. Rev. Lett. **96**, 027213 (2006).
- ³² P. Sindzingre, N. Shannon and T. Momoi, J. Magn. Magn. Mat. **310**, 1340 (2007).
- ³³ B. Schmidt, N. Shannon, and P. Thalmeier, J. Phys.: Condens. Matter **19**, 145211 (2007).
- ³⁴ B. Schmidt, N. Shannon, and P. Thalmeier, J. Magn. Magn. Mater. **310**, 1231 (2007).
- ³⁵ J. R. Viana and J. R. de Sousa, Phys. Rev. B **75**, 052403 (2007).
- ³⁶ P. Sindzingre, L. Seabra, N. Shannon, and T. Momoi, J. Phys.: Conf. Ser. **145**, 012048 (2009).
- ³⁷ P. Sindzingre, N. Shannon, and T. Momoi, J. Phys.: Conf. Ser. **200**, 022058 (2010).
- ³⁸ M. Härtel, J. Richter, D. Ihle, and S.-L. Drechsler, Phys. Rev. B **81**, 174421 (2010).
- ³⁹ J. Richter, R. Darradi, J. Schulenburg, D. J. J. Farnell, and H. Rosner, Phys. Rev. B **81**, 174429

- (2010).
- ⁴⁰ W. Nunes, J. R. Viana, and J. R. de Sousa, J. Stat. Mech. P05016 (2011).
- ⁴¹ R. Shindou, S. Yunoki, and T. Momoi, Phys. Rev. B **84**, 134414 (2011).
- ⁴² F. Wang, Phys. Rev. B **82**, 024419 (2010).
- ⁴³ S. Okumura, H. Kawamuro, T. Okubo, and Y. Motome, J. Phys. Soc. Jpn. **79**, 114705 (2010)
- ⁴⁴ D. C. Cabra, C. A. Lamas, and H. D. Rosales, Phys. Rev. B **83**, 094506 (2011).
- ⁴⁵ J. B. Fouet, P. Sindzingre, and C. Lhuillier, Eur. Phys. J. B **20**, 241 (2001).
- ⁴⁶ Z. Noorbakhsh, F. Shahbazi, S. A. Jafari, and G. Baskaran, J. Phys. Soc. Jpn. **78**, 054701 (2009).
- ⁴⁷ H. Y. Yang and K. P. Schmidt, Europhys. Lett. **94**, 17004 (2011).
- ⁴⁸ A. F. Albuquerque, D. Schwandt, B. Hetényi, S. Capponi, M. Mambrini, and A. M. Läuchli, Phys. Rev. B **84**, 024406 (2011).
- ⁴⁹ J. Reuther, D. A. Abanin, and R. Thomale, Phys. Rev. B **84**, 014417 (2011).
- ⁵⁰ J. Oitmaa and R. R. P. Singh, Phys. Rev. B **84**, 094424 (2011).
- ⁵¹ S. Okubo, F. Elmasry, W. Zhang, M. Fujisawa, T. Sakurai, H. Ohta, M. Azuma, O. A. Sumirnova, and N. Kumada, J. Phys.: Conf. Ser. **200**, 022042 (2010).
- ⁵² A. Kitaev, Ann. Phys. (N.Y.) **321**, 2 (2006); G. Baskaran, S. Mandal, and R. Shankar, Phys. Rev. Lett. **98**, 247201 (2007); J. Chaloupka, G. Jackeli, and G. Khaliullin, *ibid.* **105**, 027204 (2010)
- ⁵³ A. H. Castro Neto, F. Guinea, N. M. R. Peres, K. S. Novoselov, and A. K. Geim, Rev. Mod. Phys. **81**, 109 (2009).
- ⁵⁴ Z. Y. Meng, T. C. Lang, S. Wessel, F. F. Assaad, and A. Muramatsu, Nature **464**, 847 (2010).
- ⁵⁵ D. J. J. Farnell, R. F. Bishop, P. H. Y. Li, J. Richter, and C. E. Campbell, Phys. Rev. B **84**, 012403 (2011).
- ⁵⁶ J. Reuther, P. Wölfle, R. Darradi, W. Brenig, M. Arlego, and J. Richter, Phys. Rev. B **83**, 064416 (2011).
- ⁵⁷ H. Feldner, D. C. Cabra, and G. L. Rossini, Phys. Rev. B **84**, 214406 (2011).
- ⁵⁸ A. Mattsson, P. Fröjdh, and T. Einarsson, Phys. Rev. B **49**, 3997 (1994).
- ⁵⁹ E. Rastelli, A. Tassi, and L. Reatto, Physica **97B**, 1 (1979).
- ⁶⁰ R. F. Bishop, Theor. Chim. Acta **80**, 95 (1991).
- ⁶¹ C. Zeng, D. J. J. Farnell, and R. F. Bishop, J. Stat. Phys. **90**, 327 (1998).

- ⁶² D. J. J. Farnell and R. F. Bishop, in *Quantum Magnetism*, edited by U. Schollwöck *et al.*, Lecture Notes in Physics **645** (Springer-Verlag, Berlin, 2004), p.307.
- ⁶³ D. J. J. Farnell, R. F. Bishop, and K. A. Gernoth, Phys. Rev. B **63**, 220402(R) (2001).
- ⁶⁴ S. E. Krüger, J. Richter, J. Schulenburg, D. J. J. Farnell, and R. F. Bishop, Phys. Rev. B **61**, 14607 (2000).
- ⁶⁵ D. Schmalfuß, R. Darradi, J. Richter, J. Schulenburg, and D. Ihle, Phys. Rev. Lett. **97**, 157201 (2006).
- ⁶⁶ R. Darradi, J. Richter, and D. J. J. Farnell, Phys. Rev. B **72**, 104425 (2005).
- ⁶⁷ D. J. J. Farnell, J. Richter, R. Zinke, and R. F. Bishop, J. Stat. Phys. **135**, 175 (2009).
- ⁶⁸ R. F. Bishop, P. H. Y. Li, D. J. J. Farnell, and C. E. Campbell, Phys. Rev. B **79**, 174405 (2009).
- ⁶⁹ R. F. Bishop, P. H. Y. Li, D. J. J. Farnell, and C. E. Campbell, Phys. Rev. B **82**, 024416 (2010).
- ⁷⁰ R. F. Bishop, P. H. Y. Li, D. J. J. Farnell, and C. E. Campbell, Phys. Rev. B **82**, 104406 (2010).
- ⁷¹ R. F. Bishop and P. H. Y. Li, Eur. Phys. J. B **81**, 37 (2011).
- ⁷² We use the program package CCCM of D. J. J. Farnell and J. Schulenburg, see <http://www-e.uni-magdeburg.de/jschulen/ccm/index.html>.
- ⁷³ R. Darradi, J. Richter, and D. J. J. Farnell, Phys. Rev. B **72**, 104425 (2005).
- ⁷⁴ R. F. Bishop, D. J. J. Farnell, S. E. Krüger, J. B. Parkinson, J. Richter, and C. Zeng, J. Phys.: Condens. Matter **12**, 6887 (2000).
- ⁷⁵ H. J. Schulz and T. A. L. Ziman, Europhys. Lett. **18**, 355 (1992); H. J. Schulz, T. A. L. Ziman, and D. Poilblanc, J. Phys. I **6**, 675 (1996).
- ⁷⁶ Ch. Waldtmann, H.-U. Everts, B. Bernu, C. Lhuillier, P. Sindzingre, P. Lecheminant, and L. Pierre, Eur. Phys. J. B **2**, 501 (1998).
- ⁷⁷ J. Richter and J. Schulenburg, Eur. Phys. J. B **73**, 117 (2010).
- ⁷⁸ H. Nakano and T. Sakai, J. Phys. Soc. Jpn. **80**, 053704 (2011).
- ⁷⁹ F. Heidrich-Meisner, A. Honecker, and T. Vekua, Phys. Rev. B **74**, 020403(R) (2006).
- ⁸⁰ H. T. Lu, Y. J. Wang, Shaojin Qin, and T. Xiang, Phys. Rev. B **74**, 134425 (2006).
- ⁸¹ M. Härtel, J. Richter, D. Ihle, and S.-L. Drechsler, Phys. Rev. B **78**, 174412 (2008).
- ⁸² T. Momoi, P. Sindzingre, and N. Shannon, Phys. Rev. Lett. **97**, 257204 (2006).
- ⁸³ L. Kecke, T. Momoi, and A. Furusaki, Phys. Rev. B **76**, 060407 (2007).
- ⁸⁴ J. Sudan, A. Luscher, and A. M. Läuchli, Phys. Rev. B **80**, 140402(R) (2009).
- ⁸⁵ S. Nishimoto, S.-L. Drechsler, R. O. Kuzian, J. van den Brink, J. Richter, W. E. A. Lorenz,

Y. Skouraki, R. Klingeler, and B. Blichner, Phys. Rev. Lett. **107**, 097201 (2011).